Research Article

Shenao Cui, Ting Wang, Zhaochuan Zhang, Xiao Sun, Jiahui Li, Bangxiang Li, Weishen Zhang, Tian Su*, and Fubo Cao*

Frost resistance and life prediction of recycled brick aggregate concrete with waste polypropylene fiber

https://doi.org/10.1515/rams-2023-0154
received February 13, 2023; accepted November 13, 2023

Abstract: Due to recycled aggregate concrete technology, sustainable resource utilization can be achieved, but the weak frost resistance of this type of concrete affects its application in cold regions. Using waste polypropylene fibers as reinforcing materials can improve the mechanical properties and durability of concrete. This study explores the influence of waste polypropylene fiber on the frost resistance durability and microstructure of recycled brick aggregate (RA) concrete. The results show that with the increase in freeze–thaw cycles, the mass of the concrete first increases and then decreases, while its relative dynamic elastic modulus and compressive strength gradually decrease. After 60 freeze–thaw cycles, the maximum mass loss, maximum relative dynamic elastic modulus loss, and maximum compressive strength loss of the RA concrete are 1.73, 45.1, and 73.7%, respectively. Waste fiber (WF) can improve the frost resistance of concrete, as demonstrated by the obvious reduction in mass loss, relative dynamic elasticity modulus loss, and compressive strength loss, which are 0.11, 33.0, and 64.0%, respectively, after 60 freeze–thaw cycles. The action mechanism of WF on the frost resistance of RA concrete is revealed, and the life prediction model of RA concrete with WF under freeze–thaw conditions is established.

Keywords: recycled concrete, waste fiber, relative dynamic elastic modulus, frost resistance, life prediction model

1 Introduction

In recent years, the environmental pollution caused by construction waste has become increasingly serious [1]. Recycled concrete has gradually attracted the attention of scholars for its environmentally protective and cost-saving advantages [2]. The surface of recycled aggregate is attached to old cement mortar, which makes the interface transition zone (ITZ) more complex, and some initial microcracks are generated during the crushing process of the recycled aggregate, giving recycled concrete lower mechanical properties and durability than ordinary concrete [3]. Most research on recycled concrete has mainly concentrated on recycled stone aggregate concrete [4,5]. Waste brick is also the main component of construction waste [6]. Therefore, research on recycled brick aggregate (RA) concrete is also of great significance.

Due to the lower strength of waste bricks, more serious internal damage is generated during the crushing process, resulting in more microcracks inside the brick aggregate [7]. Through studying the mechanical properties of RA concrete, it was found that when the replacement rate of brick coarse aggregate was small, its effect on compressive strength was not significant [8], and its effect on splitting tensile strength and flexural strength was negligible [9]; when the replacement rate of brick coarse aggregate was greater than a certain degree, the mechanical properties of the concrete were significantly reduced [10,11], but compared with the compressive strength, the splitting tensile strength and flexural strength changed relatively little [12]. Moreover, the effect of brick aggregate on the mechanical

* **Corresponding author: Tian Su**, Department of Civil Engineering, School of Civil Engineering and Geomatics, Shandong University of Technology, Zibo, Shandong, 255000, China; Department of Architectural Engineering, School of Civil Engineering, Wuhan University, 8 Donghu South Road, Wuhan, Hubei, 430072, China; China Railway 11 Bureau Group Co., Ltd, 277 Zhongshan Road, Wuhan, Hubei, 430061, China; Department of Engineering and Management, International College, Krirk University, 3 Soi Ramintra 1, Ramintra Road, Anusaowaree, Bangkhen, Bangkok 10220, Thailand, e-mail: sutian@sdut.edu.cn
* **Corresponding author: Fubo Cao**, Department of Architectural Engineering, School of Civil Engineering, Inner Mongolia University of Science and Technology, 7 Alding Street, Baotou, Inner Mongolia, 014010, China, e-mail: caofubo@imust.edu.cn
Shenao Cui, Ting Wang, Zhaochuan Zhang, Xiao Sun, Jiahui Li, Bangxiang Li, Weishen Zhang: Department of Civil Engineering, School of Civil Engineering and Geomatics, Shandong University of Technology, Zibo, Shandong, 255000, China

properties of low water/cement ratio concrete was greater than that with a high water/cement ratio [13].

In the middle and high latitudes, concrete buildings often suffer from freeze–thaw damage [14]. The solution volume inside the concrete increases continuously after freezing. When the pore solution volume exceeds 91%, the pressure generated by the solution freezing causes damage to the concrete [15], degrading its mechanical properties and durability [16] and thereby affecting the normal use of the building [17]. After freeze–thaw cycles, the compressive strength and relative dynamic elastic modulus of concrete show a downwards trend [18]. The higher water absorption rate of recycled aggregate seriously affects the frost resistance durability of recycled concrete. After freeze–thaw cycles, the compressive strength, mass loss, and relative dynamic elastic modulus of recycled concrete decrease more than those of ordinary concrete [19], and the decrease degree increases with an increased recycled aggregate replacement rate [20,21]. Zaharieva *et al.* [22] found that during the freeze–thaw process, recycled aggregates discharge their internal water into the surrounding cement mortar, which is the main reason for the more severe freeze–thaw damage in recycled aggregate concrete. Hu and Wu [23] conducted a study on the salt frost resistance of recycled aggregate concrete and found that its resistance in salt water was inferior to that in fresh water. Some scholars have also found that the frost resistance of recycled aggregate concrete is equivalent to that of ordinary aggregate concrete. Yildirim *et al.* [24] found that when the replacement rate of recycled aggregate was 50%, the frost resistance of recycled concrete was not inferior to that of its ordinary counterpart. Richardson *et al.* [25] screened and washed recycled aggregates and found that the frost resistance of the concrete prepared using them was even better than that of ordinary concrete. In addition, Gokce *et al.* [26] found through experiments that the frost resistance of recycled concrete was significantly improved when using waste concrete containing air-entraining agents to prepare recycled aggregates. To date, scholars have carried out a great deal of research on the mechanical properties and frost resistance of recycled stone aggregate concrete [27], while research on RA concrete is relatively scarce.

Since the beginning of its industrial production, polypropylene fiber has been widely used in the field of clothing fabrics due to its light weight, high strength, and stability [28,29]. In recent years, the treatment of waste textiles with polypropylene fiber as the main raw material has also begun to attract attention. If waste fiber (WF) is added to recycled concrete as a reinforcing material [30], it can not only effectively improve the mechanical properties and durability [31], but also solve the problem of waste textile treatment. Through experimental research, it was found that fiber length and content had an impact on the mechanical properties of recycled concrete [32,33]. The compressive strength of WF recycled concrete with a fiber length of 30 mm and fiber content of 0.12% was found to be the best; the splitting tensile strength of that with a fiber length of 19 mm and fiber content of 0.12% was the best [34]. The impact of WF on the early strength of the concrete was more significant. Its compressive strength at an early age was higher than that of ordinary concrete with the same concrete mix ratio, while its 28 days compressive strength was slightly lower than that of ordinary concrete. This is due to the crack resistance effect of WF, which improves the early strength of WF recycled concrete [35]. The WF also affected the size effect of the concrete. With the increase in the WF content, the size effect phenomenon showed a trend of decreasing first and then increasing [36].

In addition, the incorporation of WF could also improve the durability of recycled concrete [37]. After adding WF, the chloride ion erosion resistance of this concrete is improved. With the increase in WF content, the chloride ion content shows a downwards trend [38]. It has also been found that adding a proper amount of WF could hinder the development of internal cracks and improve the frost resistance of recycled concrete. However, if too much WF is mixed, it would be unevenly distributed inside the concrete, increasing the number of harmful voids and weak interfaces, which would hinder the frost resistance [39].

At present, there are relatively few studies on the frost resistance of recycled concrete with WF, and most of them fail to clarify the mechanism involved. In addition, the existing research mostly focuses on the mechanical properties and durability of recycled stone aggregate concrete with WF, with research on applying WF in RA concrete being relatively scarce. Intending to improve RA concrete's frost resistance and realize its application in cold areas, in this study, we conducted in-depth research on the frost resistance durability of such concrete with WF, exploring the influence and action mechanism of this fiber on the concrete's frost resistance and microstructure through microstructure analysis. Based on the Weibull distribution theory, a life prediction model of WF RA concrete under freeze–thaw conditions was established. This study provides a new idea for improving the frost resistance of this type of concrete through the addition of WFs, and it could provide a theoretical basis and technical support for applying such concrete in cold regions and promoting the widespread application of recycled concrete in practical engineering.

2 Experimental overview

2.1 Raw materials

P.O 42.5 Ordinary Portland Cement applied in this study met the requirements of GB175-2007 [40]. The specific surface area of the cement was 344 m^{-2}·kg; the 3 days and 28 days compressive strengths were 22.2 and 47.3 MPa, respectively. The 3 days and 28 days flexural strengths were 4.9 and 7.8 MPa, respectively. The natural coarse aggregate (NA) was crushed stone collected from Zibo City. RA was obtained through crushing, cleaning, and grading waste bricks. The particle size of the NA and RA ranged from 5 to 25 mm; their crush index was 8.70 and 27.90%, respectively; and their water absorption was 1.10 and 16.50%, respectively. The fineness modulus of the fine aggregate used in this study was 2.9, and the water absorption was 3.1%. The waste polypropylene carpet was manually cut into 19 mm test WF, as shown in Figure 1.

2.2 Mix proportion

The concrete mix proportion is shown in Table 1. It should be noted that the RA needed to reach the saturated surface dry state before use. To ensure the uniform distribution of WFs in the concrete, the dry mixing method was adopted in this experiment: First, the sand and coarse aggregate were loaded into the mixer for dry mixing for 1 min, and then mixed with cement and WFs for 5 min. Finally, water was added and fully stirred for 5 min.

2.3 Frost resistance test program

According to the GB/T 50082-2009 Standard for Test Methods of Long-term Performance and Durability of Ordinary Concrete [41], the freeze–thaw cycle test of concrete prism specimens (100 mm × 100 mm × 400 mm) and concrete cube specimens (100 mm × 100 mm × 100 mm) was carried out using a rapid freeze–thaw cycle test machine (Figure 2). For the study, three replicate test specimens were prepared under different freeze–thaw cycles. The relative dynamic elastic modulus and mass loss of the concrete prism specimens under different freeze–thaw cycles were tested with a DT-10 W dynamic elastic modulus tester (Figure 3) and an electronic scale with a maximum range of 30 kg. The compressive strength of the concrete cube specimens under different freeze–thaw cycles was tested with a microcomputer-controlled electrohydraulic servo pressure testing machine (Figure 4).

Table 1: Concrete mix design (kg·m^{-3})

Specimen	Water	Cement	Sand	NA	RA	WF
P [44]	175	350	700	1,140	0	—
B50	175	350	700	570	468	—
B100	175	350	700	0	936	—
X2B50	175	350	700	570	468	1.092
X2B100	175	350	700	0	936	1.092

where P is ordinary concrete; B is RA concrete; B50 is recycled concrete with 50% brick aggregate; and X2B50 is recycled concrete with 50% RA and 2% (volume content) WF.

2.4 Microstructure test program

The concrete specimens used for microscopic tests were placed in an oven for 24 h (60°C) and then observed under a Quanta 250 FEG field emission environmental scanning electron microscope (SEM), as shown in Figure 5. The specific process was as follows: First, the RA concrete specimens to be tested with a size of 10 mm × 10 mm × 10 mm were placed under an SEM.

Figure 1: WF.

Figure 2: Freeze–thaw cycle test machine.

Figure 3: Dynamic elastic modulus tester.

3 Results and discussion

3.1 Apparent phenomenon after freeze–thaw cycle

The apparent phenomenon and general microscope observation image of the concrete after the freeze–thaw cycle are shown in Figures 6 and 7, respectively. It can be seen that before the freeze–thaw cycle, the surface of the concrete specimen was smooth, and there was no obvious difference between each group of specimens. After ten freeze–thaw cycles, a small amount of cement mortar fell off, and there were small holes in each group. The peeling phenomenon was not significant, and the apparent phenomenon of different concrete was not significantly different. After 30 freeze–thaw cycles, the number of small

Figure 4: Electrohydraulic servo pressure testing machine.

holes in the ordinary concrete specimen increased, and the coarse aggregate was exposed; the surface of the recycled concrete specimen with a 50% RA replacement rate became rough with densely distributed small holes, and the amount of mortar falling off increased. The recycled concrete specimen with a 100% RA replacement rate had relatively more surface holes than that with a 50% replacement rate. After 50 freeze–thaw cycles, the apparent phenomena of the ordinary concrete and RA concrete specimens were significantly different. The aggregate exposure speed of the ordinary concrete specimens was significantly faster, while the number of small holes on the surface of the RA concrete specimens was higher. The apparent phenomena of the recycled concrete specimen with a 100% RA replacement rate were similar to those with a 50% replacement rate, but the number of small holes on the surface of the former

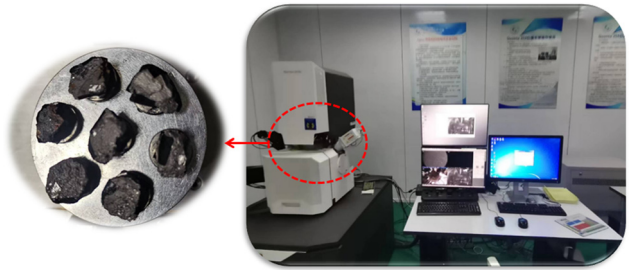

Figure 5: Microstructure test.

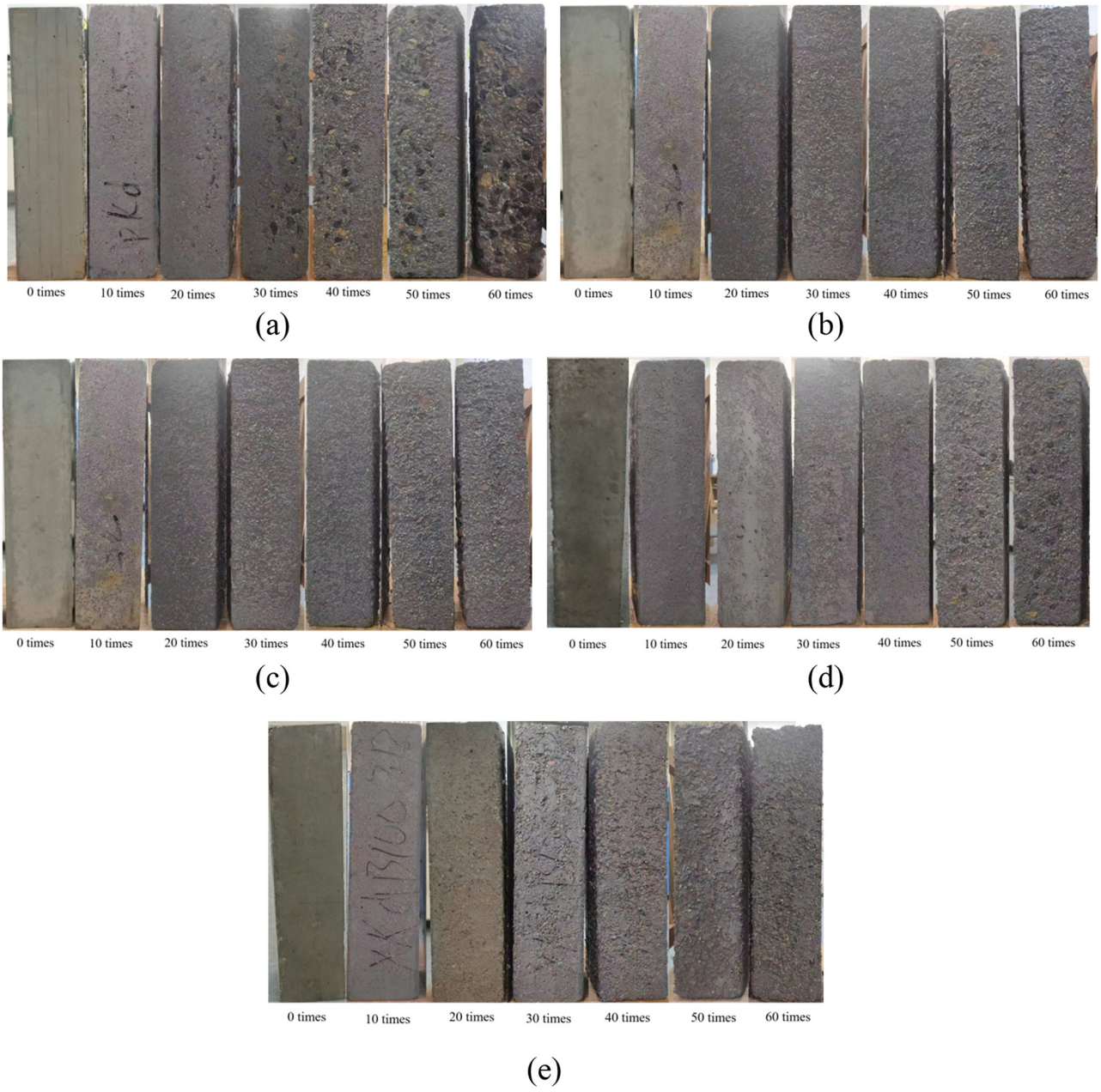

Figure 6: Apparent phenomena after freeze–thaw cycle. (a) P [44], (b) B50 [44], (c) B100, (d) X2B50, and (e) X2B100.

specimen was higher. The reason why the freeze–thaw damage of ordinary concrete is more serious than that of recycled concrete may be related to the different locations of the damage. According to the theory of hydrostatic [42] and osmotic pressure [43], when the freeze–thaw cycle occurs, the large hole in the connecting hole will absorb the water from the small hole, thus squeezing the wall of the large hole. For ordinary concrete, the hole in the ITZ is large, so freeze–thaw failure occurs in the ITZ first. For RA concrete, due to its large water absorption, the water in the ITZ will enter the aggregate during the freeze–thaw cycle, relieving the pressure in this zone. Moreover, the surface of RA is rougher than that of ordinary aggregate, and many pores and cracks make the cement slurry flow into the brick aggregate and integrate, making the bond strength of the RA and cement stone better than that of ordinary aggregate and cement stone.

In addition, when the number of freeze–thaw cycles was small, there was no significant difference in the surface damage between the RA concrete with and without WF; after 50 freeze–thaw cycles, the phenomenon of cement mortar falling off and aggregate becoming exposed on the

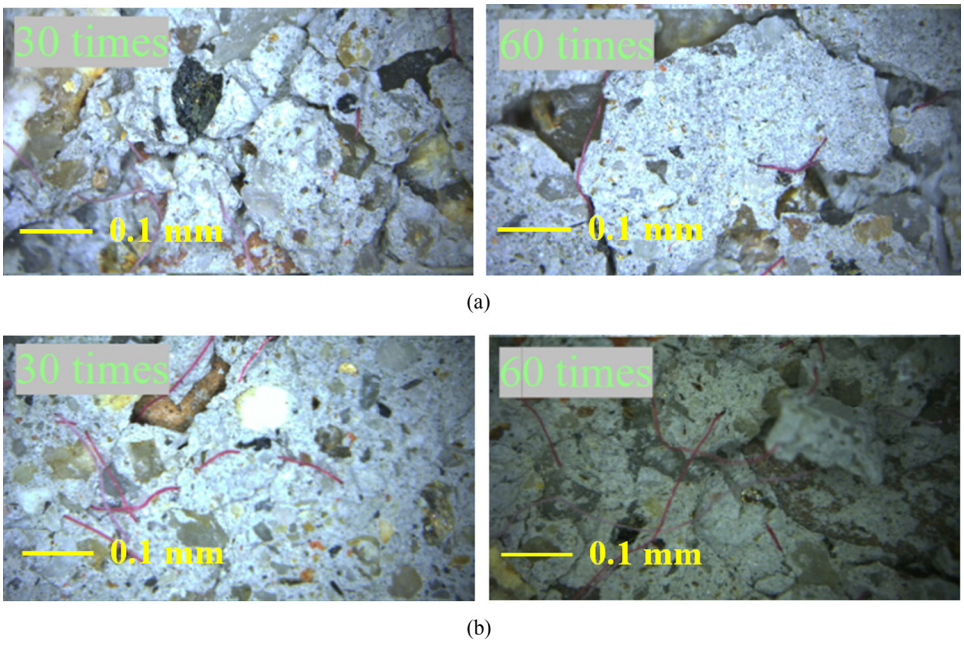

Figure 7: General microscope observation images after freeze–thaw cycle (zoom in 100×). (a) X2B50 and (b) X2B100.

surface of the specimen was weaker in the RA concrete with WF. This is because the fiber forms a three-dimensional network structure after being uniformly dispersed in concrete, which can optimize the pore structure and strengthen the connection performance and overall stability of each part of the cement stone, thus enhancing the frost resistance of RA concrete. Figure 7 shows that the WF formed a three-dimensional network structure after being evenly dispersed in the concrete, forming with the cement stone a whole unit, thus preventing the stone from falling off the surface of the specimen. This greatly hindered the secondary loss caused by the expansion of freeze–thaw pores triggered by the cement stone falling off the concrete surface.

3.1.1 Mass loss

The relationship between the mass loss of concrete specimens and the number of freeze–thaw cycles is shown in Figure 8. It can be seen that the mass of the specimens first increased and then decreased; after 60 freeze–thaw cycles, the mass loss of RA concrete was 1.13–1.73%. The reasons for this increase in the early stage of the freeze–thaw cycle are as follows: When the temperature drops, the water inside the concrete specimen begins to freeze, resulting in a gradual increase in the hydrostatic and osmotic pressure inside the specimen. When the pressure stress on the inner wall of the pore reaches a certain degree, internal microcracks begin to occur. In the freeze–thaw cycle, water enters the specimen through the microcracks, increasing the mass of concrete. When the number of cycles was small, the mass of water entering the specimens was greater than their mass loss, thus increasing the specimens' mass [45]. With the increase in the number of freeze–thaw cycles, the mortar on the surface of the concrete specimen continued to peel off, and the fine aggregate was lost, increasing the mass loss of the specimens.

It can also be seen from Figure 8 that after 60 freeze–thaw cycles, the mass loss of the RA concrete specimens was larger than that of its counterpart without WF, which

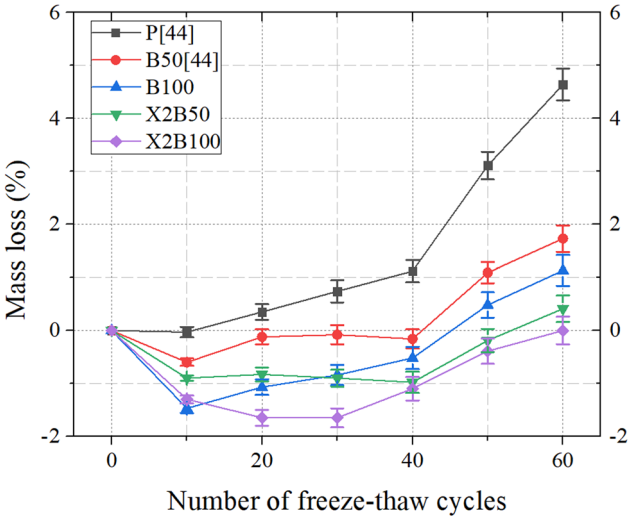

Figure 8: Mass loss after freeze–thaw cycle.

was 0.11–0.41%. WF could improve the frost resistance of RA concrete by improving the tensile strength of the concrete [46], which could better reduce the peeling of mortar on the concrete surface and reduce the mass loss.

3.1.2 Relative dynamic elasticity modulus

The relationship between the relative dynamic elastic modulus of the concrete specimens and the number of freeze–thaw cycles is shown in Figure 9. The modulus showed a downwards trend after the freeze–thaw cycles. After 60 freeze–thaw cycles, the modulus of the ordinary aggregate concrete, 50% RA concrete, and 100% RA concrete decreased by 48.0, 40.1, and 45.1%, respectively. This is because as the number of freeze–thaw cycles increases, the freeze–thaw damage of concrete continues to increase, resulting in more loose material inside the concrete.

The relative dynamic elastic modulus loss of RA concrete with WF was lower than that of its counterpart without WF. After 60 freeze–thaw cycles, the relative dynamic elastic modulus of the 50% RA concrete specimens with WF was 17.8% higher than that of the specimens without WF; the relative dynamic elastic modulus of the 100% RA concrete specimens with WF was 21.8% higher than that of the specimens without WF. It can be seen that the WF with a 2% content can improve the frost resistance of RA concrete and slow down the decrease rate of the relative dynamic elastic modulus. The reason for this is that the appropriate amount of WF can prevent cracks, effectively control the development of microcracks, increase the air content to a certain extent, and improve the pore structure, altogether improving the frost resistance of RA concrete. This is consistent with the conclusions of Huo *et al.* [47] and Xue and Li [48].

3.1.3 Compressive strength

The relationship between the compressive strength of concrete specimens and the number of freeze–thaw cycles is shown in Figure 10. With the increase in the number of freeze–thaw cycles, the compressive strength of each concrete group gradually decreased. When the number of freeze–thaw cycles was small, the compressive strength loss of the RA concrete was larger than that of the ordinary concrete. After 30 freeze–thaw cycles, the compressive strength of the ordinary aggregate concrete, 50% RA concrete, and 100% RA concrete decreased by 30.1, 39.7, and 55.5%, respectively. With the increase in freeze–thaw cycles, the compressive strength loss of the RA concrete was lower than that of the ordinary concrete. After 60 freeze–thaw cycles, the compressive strength of the ordinary aggregate concrete, 50% RA concrete, and 100% RA concrete decreased by 83.2, 68.9, and 73.7%, respectively. The reason for this is that when the number of freeze–thaw cycles is small, the porosity of concrete plays a major role in the frost resistance of the specimen. According to the basic performance of the aggregate, the water absorption of RA was 15 times that of stone aggregate (water absorption of NA and RA were 1.10 and 16.50%, respectively), indicating that the internal porosity of RA was higher. With the continuous increase in the RA replacement rate, the total volume of concrete pores continues to increase, and the effective water/cement ratio continues to increase, which reduces the frost resistance. With the increase in freeze–thaw cycles, a large amount of

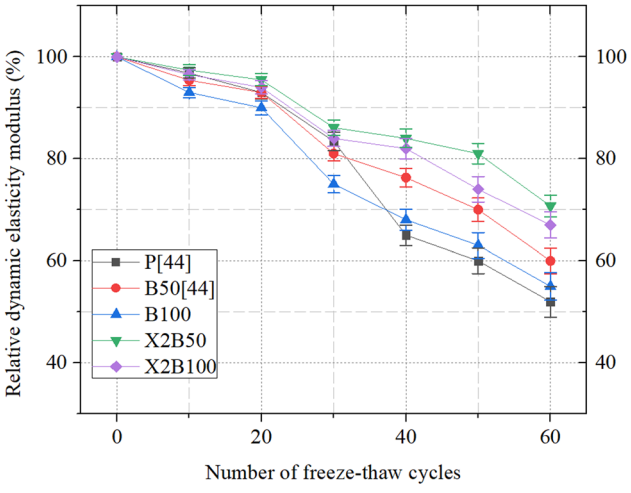

Figure 9: Relative dynamic elasticity modulus after freeze–thaw cycle.

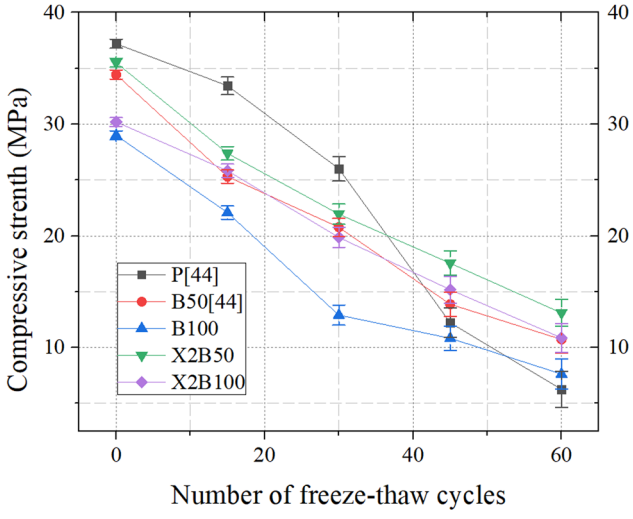

Figure 10: Concrete compressive strength after freeze–thaw cycle.

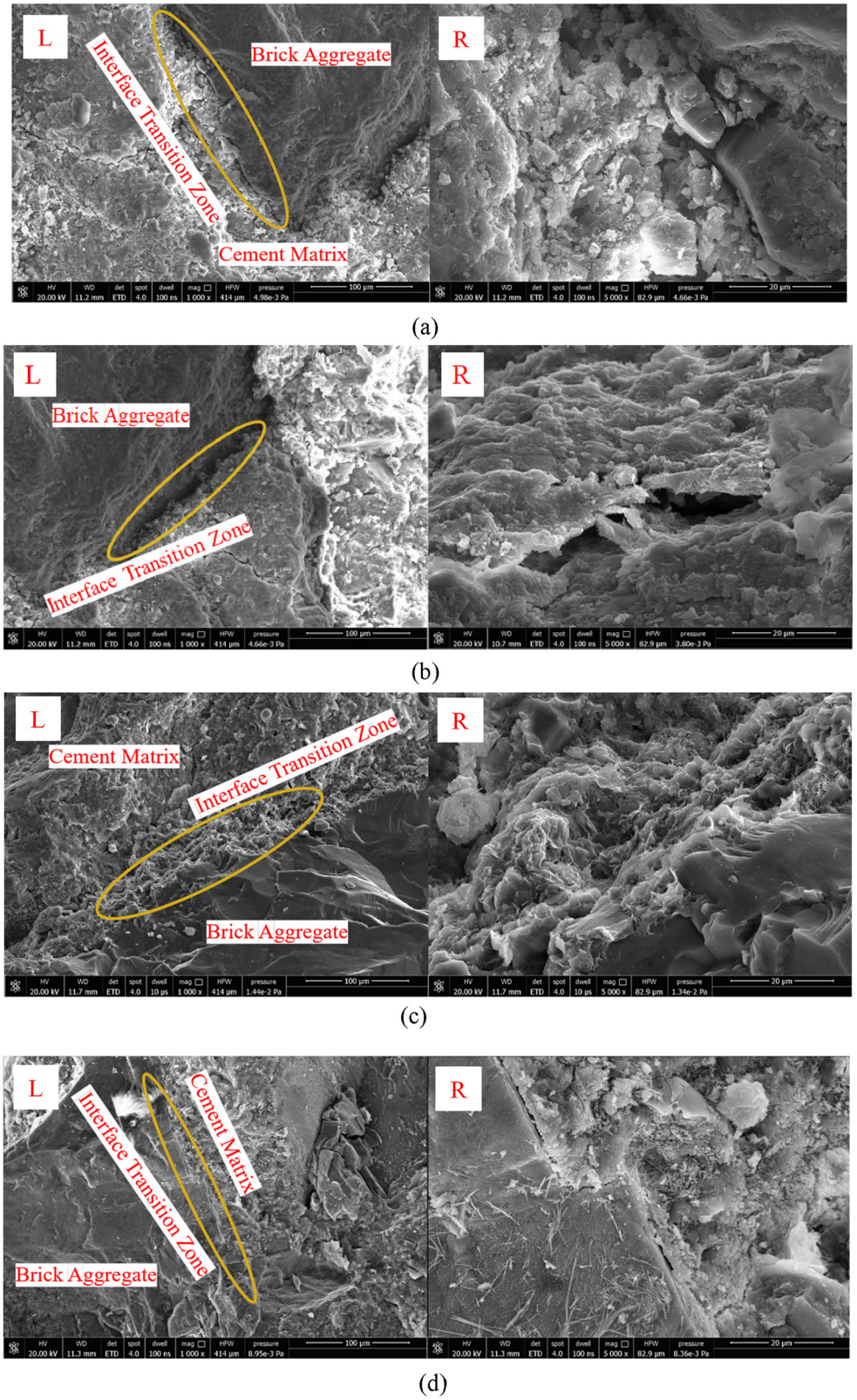

Figure 11: SEM image after freeze–thaw cycle. (a) P-15, (b) P-45, (c) B50-15, (d) B50-45, (e) X2B50-15, (f) X2B50-45, and (g) X2B50-60.

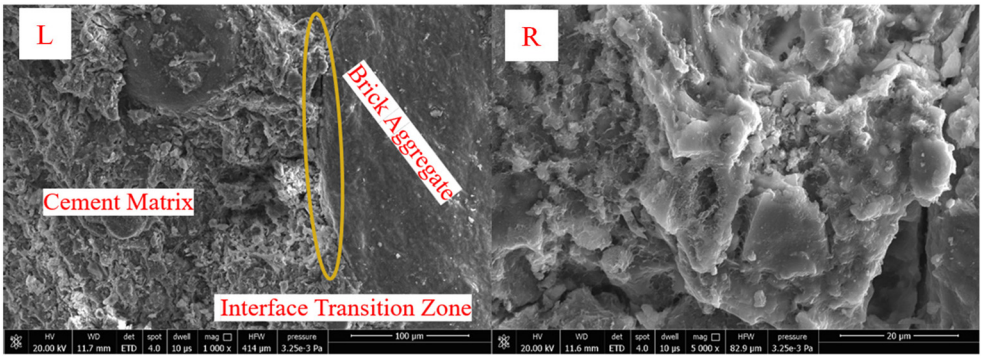

(e)

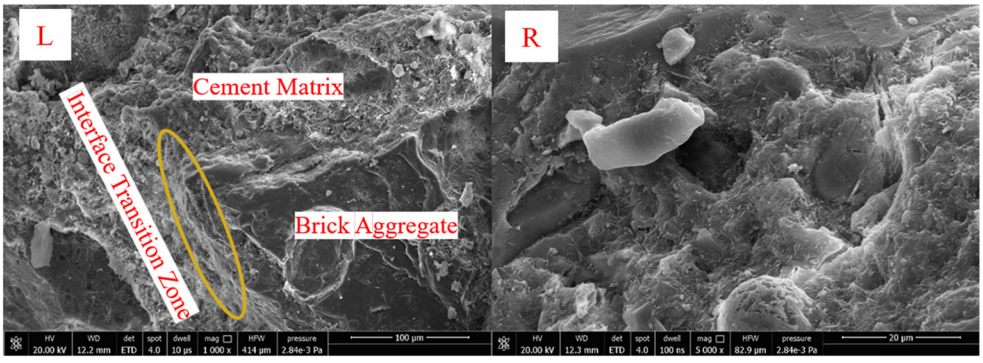

(f)

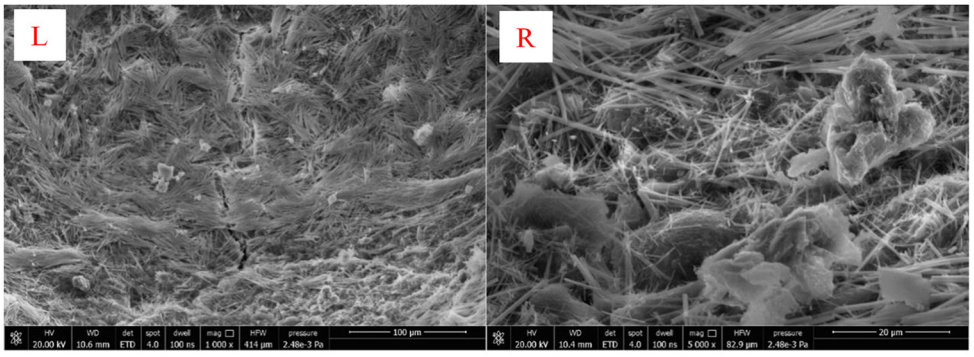

(g)

Figure 11: (*Continued*)

cement stone falls off the concrete, while the surface of RA is rough, which can better embed with the cement stone, thus reducing the cement stone falling off and lessening the resultant secondary damage. Therefore, the appropriate amount of RA can improve the frost resistance of concrete at the later stage of the freeze–thaw cycle.

It can also be seen that the WF improved the compressive strength of the RA concrete after freeze–thaw cycles. After 60 freeze–thaw cycles, the compressive strength of the 50% RA concrete specimens with WF was 22.1% higher than that of specimens without WF; the compressive strength of the 100% RA concrete specimens with WF was 42.3% higher than that of specimens without WF. In addition, the compressive strength decline curve of the WF RA concrete was close to linearity. As mentioned above, the WF formed a three-dimensional network structure after being evenly dispersed in the concrete, which slowed down the secondary damage caused by cement falling off, thus slowing down the decrease in the compressive strength of the RA concrete after the freeze–thaw cycles.

3.2 Microstructure analysis

An SEM image of the concrete after the freeze–thaw cycles is shown in Figure 11 (the picture on the left side (L) mainly

reflects the bonding between cement stone and aggregate in the ITZ; the picture on the right side (R) mainly reflects the development of cracks and holes in the ITZ or near the cement stone). It can be seen from Figure (a)–L and Figure (b)–L that with the increase in the number of freeze–thaw cycles, the volume of cement stone covering the aggregate surface in ordinary concrete decreased, which reflected that the bonding ability between the cement stone and aggregate worsened. It can be seen from Figure (a)–R and Figure (b)–R that with the increase in freeze–thaw cycles, the size of voids and cracks in the ITZ) became larger, and the filling rate of cement stone in the ITZ decreased.

Through the comparison between Figures (a)/(b) and (c)/(d), it can be seen that after the same number of freeze–thaw cycles, the bonding between aggregate and cement stone in the ITZ of RA concrete was better. This is due to the rough and uneven surface of the RA, which makes the RA and the cement stone bond well, which reduces the cement stone shedding in the ITZ after freeze–thaw cycles. It can be seen from Figures (c)–R and (d)–R that the boundary of the ITZ became more obvious after undergoing freeze–thaw cycles. There was no obvious boundary in the ITZ after 15 freeze–thaw cycles, while a clear boundary appeared after 45 freeze–thaw cycles.

From Figure (e)–(g), it can be observed that compared to RA concrete, after the same number of freeze–thaw cycles, fiber reinforced RA concrete with WF had no large voids in the cement stone, and the filling effect of hydration products on the pores was better, which was one of the reasons why WF improved the frost resistance of the RA concrete.

3.3 Freeze–thaw damage life prediction model

According to the principle of damage mechanics, the concrete material was gradually destroyed during the stress process, and the process of material damage could be studied according to the change in damage degree. In this study, the relative dynamic modulus of elasticity was used as an index to evaluate the damage degree. The damage degree D_n was defined as:

$$D_n = \frac{E_0 - E_n}{E_0}, \tag{1}$$

where E_0 is the initial dynamic elastic modulus before the freeze–thaw cycle and E_n is the dynamic elastic modulus after n freeze–thaw cycles.

In this study, a two-parameter model was used to predict the concrete life. The Weibull probability density function of concrete life (n) is as follows:

$$f(n) = \frac{b}{a}\left(\frac{n}{a}\right)^{(b-1)} \exp\left[-\left(\frac{n}{a}\right)^b\right], \tag{2}$$

where a is the scale standard and b is the shape standard. The life probability distribution function of concrete is as follows:

$$F(n) = 1 - \exp\left[-\left(\frac{n}{a}\right)^b\right]. \tag{3}$$

After n_1 freeze–thaw cycles, the failure probability of concrete is as follows:

$$P_{\mathrm{f}}(n_1) = 1 - \exp\left[-\left(\frac{n_1}{a}\right)^b\right]. \tag{4}$$

When the concrete reaches the freeze–thaw life (after n_n freeze–thaw cycles), it is considered invalid, at which point $P_{\mathrm{f}}(n_1) = 1$ and $D(n_n) = 1$. Therefore, the following can be obtained:

$$P_{\mathrm{f}}(n1) = D(nn). \tag{5}$$

From the Weibull distribution function, the reliability function can be obtained as follows:

$$R(n) = 1 - F(n) = \exp\left[-\left(\frac{n}{a}\right)^b\right] = 1 - D(n). \tag{6}$$

The Weibull transformation is performed on Eq. (6), and the logarithms on both sides can be obtained:

$$\ln\left(\ln\left(\frac{1}{R_n}\right)\right) = b(\ln(n) - \ln(a)). \tag{7}$$

Let $Y = \ln(\ln(1/R(n)))$, $X = \ln(n)$, and $C = -b\ln(a)$; then, Eq. (7) can be changed to $Y = bX + C$. If the actual concrete life conforms to the Weibull distribution, then Y and X should show a linear relationship. Through the correlation analysis of the least square method, the parameters b and C and the correlation coefficient R^2 can be obtained. If the correlation coefficient R^2 exceeds 0.9, the linear correlation between Y and X is strong; that is, the life of concrete specimens conforms to the Weibull distribution.

The actual number of freeze–thaw cycles was analyzed as an independent variable, and the Weibull distribution value of concrete life was obtained by fitting with Origin analysis software [49], as shown in Table 2. The Weibull values in Table 2 were linearly fitted to obtain the corresponding Weibull parameter values b and c, as shown in Figure 12 and Table 3. The regression relationship coefficient R^2 was greater than 0.95, indicating that the linear correlation was good; that is, the measured data satisfied the Weibull distribution. The Weibull distribution life prediction model of concrete under a freeze–thaw cycle is as follows:

Table 2: Weibull distribution values

	Freeze–thaw cycle	1/*R*(*n*)	*X* = ln(*n*)	*Y* = ln(ln(1/*R*(*n*)))
P [44]	10	1.033058	2.302585	−3.425802
	20	1.075269	2.995732	−2.623194
	30	1.199041	3.401197	−1.706379
	40	1.538462	3.688879	−0.842151
	50	1.666667	3.912023	−0.671727
	60	1.923077	4.094345	−0.424760
B50 [44]	10	1.048218	2.302585	−3.055660
	20	1.075269	2.995732	−2.623194
	30	1.234568	3.401197	−1.557220
	40	1.310616	3.688879	−1.307493
	50	1.428571	3.912023	−1.030930
	60	1.666667	4.094345	−0.671727
B100	10	1.041667	2.302585	−3.198534
	20	1.081081	2.995732	−2.551540
	30	1.282051	3.401197	−1.392468
	40	1.333333	3.688879	−1.245899
	50	1.5625	3.912023	−0.806793
	60	1.818182	4.094345	−0.514437
X2B50	10	1.026694	2.302585	−3.636516
	20	1.04712	2.995732	−3.078159
	30	1.16144	3.401197	−1.899384
	40	1.190476	3.688879	−1.746671
	50	1.234568	3.912023	−1.557220
	60	1.414427	4.094345	−1.059224
X2B100	10	1.036269	2.302585	−3.334647
	20	1.06383	2.995732	−2.782633
	30	1.190476	3.401197	−1.746671
	40	1.219512	3.688879	−1.617213
	50	1.351351	3.912023	−1.200296
	60	1.492537	4.094345	−0.915098

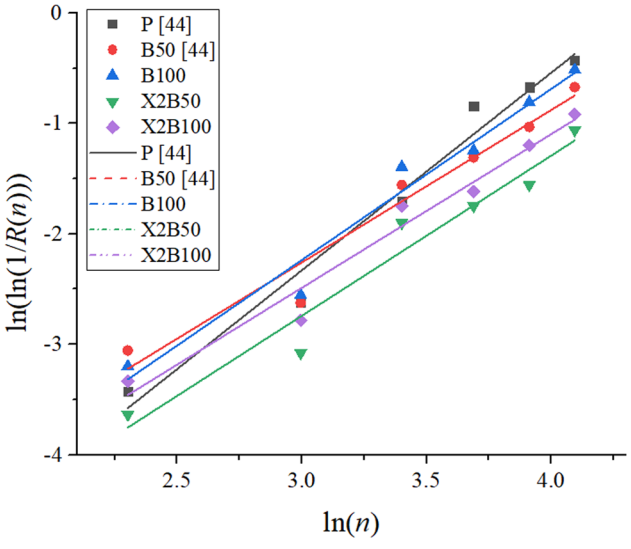

Figure 12: Weibull distribution life linear regression line.

Table 3: Weibull distribution results of concrete life

	b	*c*	R^2
P [44]	1.78883	−7.69613	0.97472
B50 [44]	1.38057	−6.40043	0.95773
B100	1.54921	−6.88425	0.96955
X2B50	1.45034	−7.09274	0.95478
X2B100	1.39152	−6.66270	0.96751

P [44]:

$$Y = \ln(\ln(1/R(n))) = 1.78883\ln(n) - 7.69613. \quad (8)$$

B50 [44]:

$$Y = \ln(\ln(1/R(n))) = 1.38057\ln(n) - 6.40043. \quad (9)$$

B100:

$$Y = \ln(\ln(1/R(n))) = 1.54921\ln(n) - 6.88425\ . \quad (10)$$

X2B50:

$$Y = \ln(\ln(1/R(n))) = 1.45034\ln(n) - 7.09274. \quad (11)$$

X2B100:

$$Y = \ln(\ln(1/R(n))) = 1.39152\ln(n) - 6.66270. \quad (12)$$

When the relative dynamic elastic modulus was reduced to 60%, the concrete member could be judged as a failure. By substituting "*R*(*n*) = 0.6" in Eqs. (8)–(12), it can be concluded that the ultimate freeze–thaw cycles of ordinary aggregate concrete, 50%-replacement-rate RA concrete, 100%-replacement-rate RA concrete, 50%-replacement-rate RA concrete with WF, and 100%-replacement-rate RA concrete with WF are 50, 63, 55, 83, and 74, respectively. The incorporation of RA could improve the frost resistance life of concrete, but the improvement effect decreased with the increase in the brick aggregate replacement rate. When the replacement rate of RA was 50%, the service life of concrete was increased by 26.0%. When the replacement rate of RA is 100%, the life of concrete is increased by 10.0%. In addition, WFs could improve the frost resistance life of RA concrete. The WFs with 2% content could improve the freeze–thaw damage life of 50 and 100%-replacement-rate RA concrete by 31.7 and 34.5%, respectively.

4 Conclusions

1) Before the freeze–thaw cycle, the surface of the concrete specimen was smooth, and there was no obvious difference between each group of concrete specimens. With the increase in the number of freeze–thaw cycles, the surface of the concrete specimen exhibited cement

mortar peeling, and then the aggregate was exposed and fell off.

2) With the increase in the number of freeze–thaw cycles, the mass of concrete first increased and then decreased, while the relative dynamic elastic modulus and compressive strength of concrete gradually decreased. After 60 freeze–thaw cycles, the maximum mass loss, maximum relative dynamic elastic modulus loss, and maximum compressive strength loss of RA concrete were 1.73, 45.1, and 73.7%, respectively.

3) WF could improve the frost resistance of RA concrete, which was mainly manifested in the obvious reduction in cement mortar peeling and aggregate exposure and the reduction in mass loss, relative dynamic elasticity modulus loss, and compressive strength loss. After 60 freeze–thaw cycles, the maximum mass loss, maximum compressive strength loss, and maximum relative dynamic elastic modulus loss of RA concrete with WF are 0.11, 33.0, and 64.0%, respectively.

4) WF formed a three-dimensional network structure after being evenly dispersed in the concrete, forming with the cement stone a whole unit, thus preventing the cement stone from falling off the surface of the specimen. In addition, WF could change the internal pore structure, making the filling effect of small hydration products in WF concrete specimens on pores better.

5) Based on the Weibull distribution theory, a life prediction model of WF RA concrete under a freeze–thaw environment was established. WF could improve the freeze–thaw damage life of 50% RA replacement rate concrete by 31.7% and improve the freeze–thaw damage life of 100% RA replacement rate concrete by 34.5%.

According to the research results of this study, WFs can improve the frost resistance of RA concrete, and the good bond performance between concrete and steel bars is the foundation of their collaborative action. Therefore, the bond performance between WF RA concrete and steel bars in freeze–thaw environments is worthy of further research.

Acknowledgments: The study was carried out with the support of the China Postdoctoral Science Foundation (2022M723687); Doctoral Science and Technology Startup Foundation of Shandong University of Technology (420048); National Undergraduate Innovation and Entrepreneurship Training Program (202310433045); National Nature Science Foundation of China (51868061); and Natural Science Foundation of Inner Mongolia Autonomous Region (2020MS05071, 2022LHMS05011). In addition, thank Zibo Xintiansheng Concrete Co., Ltd.for the support of this research.

Funding information: The study was carried out with the support of the Foundation of China Postdoctoral Science Foundation (2022M723687); Doctoral Science and Technology Startup Foundation of Shandong University of Technology (420048); National Undergraduate Innovation and Entrepreneurship Training Program (202310433045); National Nature Science Foundation of China (51868061); and Natural Science Foundation of Inner Mongolia Autonomous Region (2020MS05071, 2022LHMS05011).

Author contributions: All authors have accepted responsibility for the entire content of this manuscript and approved its submission.

Conflict of interest: The authors state no conflict of interest.

Data availability statement: All data generated or analyzed during this study are included in this published article.

References

[1] Su, T., C. Wang, F. Cao, Z. Zou, C. Wang, J. Wang, et al. An overview of bond behavior of recycled coarse aggregate concrete with steel bar. *Reviews on Advanced Materials Science*, Vol. 6, No. 1, 2021, pp. 127–144.

[2] Yuan, J., J. Wu, T. Su, and D. Lin. Dynamic response of reinforced recycled aggregate concrete pavement under impact loading. *Applied Sciences*, Vol. 12, No. 17, 2022, id. 8804.

[3] Dimitriou, G., P. Savva, and M. F. Petrou. Enhancing mechanical and durability properties of recycled aggregate concrete. *Construction and Building Materials*, Vol. 158, 2018, pp. 228–235.

[4] Peng, Q., L. Wang, and Q. Lu. Influence of recycled coarse aggregate replacement percentage on fatigue performance of recycled aggregate concrete. *Construction and Building Materials*, Vol. 169, 2018, pp. 347–353.

[5] Su, T., Z. Huang, J. Yuan, Z. Zou, C. Wang, and H. Yi. Bond properties of deformed rebar in frost-damaged recycled coarse aggregate concrete under repeated loadings. *Journal of Materials in Civil Engineering*, Vol. 34, No. 10, 2022, id. 04022257.

[6] Xu, L., W. Su, and T. Su. Influence of recycled clay brick aggregate on the mechanical properties of concrete. *Reviews on Advanced Materials Science*, Vol. 61, No. 1, 2022, pp. 372–380.

[7] Wang, T., Q. S. Wang, S. A. Cui, H. H. Yi, T. Su, and Z. Y. Tan. Effects of nano-materials reinforced aggregate on mechanical properties and microstructure of recycled brick aggregate concrete. *Materials Science (MEDŽIAGOTYRA)*, Vol. 29, No. 3, 2023, pp. 347–355.

[8] Cachim, P. B. Mechanical properties of brick aggregate concrete. *Construction and Building Materials*, Vol. 23, No. 3, 2009, pp. 1292–1297.

[9] Li, W. *Experimental Study on the Effect of Recycled Coarse Aggregate on the Mechanical Properties of Recycled Concrete*, Hubei University of Technology, Wuhan, 2019. (in Chinese).

[10] Zheng, C., C. Lou, G. Du, X. Li, Z. Liu, and L. Li. Mechanical properties of recycled concrete with demolished waste concrete aggregate

and clay brick aggregate. *Results in Physics*, Vol. 9, 2018, pp. 1317–1322.
[11] Zhu, M. *Experimental study on mix proportion and basic mechanical properties of recycled brick aggregate concrete*, Xi'an University of Science and Technology, Xi'an; 2020. (in Chinese).
[12] Zhang, L., H. Z. Li, and J. L. Ren. Experimental study on compressive strength of the concrete with 100% recycled clay brick aggregates. *Concrete*, Vol. 11, 2020, pp. 79–8288. (in Chinese).
[13] Chen, H. J., T. Yen, and K. H. Chen. Use of building rubbles as recycled aggregates. *Cement and Concrete Research*, Vol. 33, No. 1, 2003, pp. 125–132.
[14] Su, T., T. Wang, C. Wang, and H. Yi. The influence of salt-frost cycles on the bond behavior distribution between rebar and recycled coarse aggregate concrete. *Journal of Building Engineering*, Vol. 45, 2022, id. 103568.
[15] Deng, X., X. Gao, R. Wang, and C. Zhao. Study on frost resistance and pore distribution change of recycled concrete. *Materials Reports*, Vol. 35, No. 16, 2021, pp. 16028–16034. (in Chinese).
[16] Su, T., J. Wu, G. Yang, and Z. Zou. Bond behavior between recycled coarse aggregate concrete and steel bar after salt-frost cycles. *Construction and Building Materials*, Vol. 226, No. 11, 2019, pp. 673–685.
[17] Huang, X. T., T. Su, J. X. Wang, Cao, F. B., and C. X. Wang. Bond performance of corroded steel reinforcement and recycled coarse aggregate concrete after freeze–thaw cycles. *Sustainability*, Vol. 15, No. 7, 2023, id. 6122.
[18] Zhu, H. B. and X. Li. Experiment on freezing and thawing durability characteristics of recycled aggregate concrete. *Key Engineering Materials*, Vol. 400, No. 10, 2009, pp. 447–452.
[19] Cao, W. L., M. B. Liang, H. Y. Dong, and J. W. Zhang. Experimental study on basic mechanical properties of recycled concrete after freeze-thaw cycles. *Journal of Natural Disasters*, Vol. 21, No. 3, 2012, pp. 184–190. (in Chinese).
[20] Ji, W. Y. *Study on bond behavior between rebar and waste fiber recycled concrete under freeze-thaw conditions*. Nanjing University of Aeronautics and Astronautics, Nanjing, 2020. (in Chinese).
[21] Cheng, Y., X. Shang, and Y. Zhang. Experimental research on durability of recycled aggregate concrete under freeze-thaw cycles. *Journal of Physics Conference Series*, Vol. 870, No. 1, 2017, pp. 1–4.
[22] Zaharieva, R., F. Buyle-Bodin, and E. Wirquin. Frost resistance of recycled aggregate concrete. *Cement and Concrete Research*, Vol. 34, No. 10, 2004, pp. 1927–1932.
[23] Hu, J., and J. Wu. Mechanical properties and uni-axial compression stress-strain relation of recycled coarse aggregate concrete subjected to salt-frost cycles. *Construction and Building Materials*, Vol. 197, No. 2, 2019, pp. 652–666.
[24] Yildirim, S. T., C. Meyer, and S. Herfellner. Effects of internal curing on the strength, drying shrinkage and freeze-thaw resistance of concrete containing recycled concrete aggregates. *Construction and Building Materials*, Vol. 91, No. 8, 2015, pp. 288–296.
[25] Richardson, A., K. Coventry, and J. Bacon. Freeze/thaw durability of concrete with recycled demolition aggregate compared to virgin aggregate concrete. *Journal of Cleaner Production*, Vol. 19, No. 2–3, 2011, pp. 272–277.
[26] Gokce, A., S. Nagataki, T. Saeki, and M. Hisada. Freezing and thawing resistance of air-entrained concrete incorporating recycled coarse aggregate: The role of air content in demolished concrete. *Cement and Concrete Research*, Vol. 34, No. 5, 2004, pp. 799–806.
[27] Liu, K., J. Yan, Q. Hu, Y. Sun, and C. Zou. Effects of parent concrete and mixing method on the resistance to freezing and thawing of air-entrained recycled aggregate concrete. *Construction and Building Materials*, Vol. 106, No. 3, 2016, pp. 264–273.
[28] Caro, M., Y. Jemaa, S. Dirar, and A. Quinn. Bond performance of deep embedment FRP bars epoxy-bonded into concrete. *Engineering Structures*, Vol. 147, 2017, pp. 448–457.
[29] Rezazadeh, M., and V. Carvelli. A damage model for high-cycle fatigue behavior of bond between FRP bar and concrete. *International Journal of Fatigue*, Vol. 111, 2018, pp. 101–111.
[30] Islam, M., K. Islam, M. Shahjala, E. Khatun, S. Islam, and A. Razzaque. Influence of different types of fibers on the mechanical properties of recycled waste aggregate concrete. *Construction and Building Materials*, Vol. 337, 2022, id. 127577.
[31] Yazdanbakhsh, A. Technical and economic implications of using recycled fiber-reinforced polymer waste as aggregate in concrete. *Waste and Byproducts in Cement-Based Materials*, Vol. 5, 2021, pp. 139–150.
[32] Zheng, C., S. Li, Y. Hou, and B. Jin. Frost resistance of fiber-reinforced self-compacting recycled concrete. *Reviews on Advanced Materials Science*, Vol. 61, No. 1, 2022, pp. 711–725.
[33] You, F., S. Luo, and J. Zheng. Experimental study on residual compressive strength of recycled aggregate concrete under fatigue loading. *Frontiers in Materials*, Vol. 9, 2022, id. 817103.
[34] Zhou, J. H., T. T. Li, and G. Z. Yang. Experimental research on mechanical properties of waste fiber recycled concrete. *Concrete*, Vol. 3, 2013, pp. 1–4. (in Chinese).
[35] Wang, Y. C. *Study on early age mechanical properties of waste fiber recycled concrete*, Shenyang Jianzhu University, Shenyang, 2020, (in Chinese).
[36] Yang, J. N. *Size effect on strength test of waste fiber recycled concrete*, Shenyang Jianzhu University, Shenyang, 2018. (in Chinese).
[37] Yue, X. J. *Experimental research on waste fiber and recycled concrete erosion resistance performance*, Shenyang Jianzhu University: Shenyang, 2013. (in Chinese).
[38] Li, H., T. Liu, X. Ding, C. Luo, and J. Mi. Ability to resist sulfate of waste fiber recycled concrete. *Concrete*, Vol. 10, 2019, pp. 18–21. (in Chinese).
[39] Wu, D. *Study on bond behavior between rebar and waste fiber recycled concrete under freeze-thaw conditions*, Shenyang Jianzhu University, Shenyang, 2020. (in Chinese).
[40] *Common Portland Cement (GB175-2007)*, China Standardization Administration, Beijing, 2007. (in Chinese).
[41] *Standard for Test Method of Mechanical Properties on Ordinary Concrete (GB/T 50081-2002)*. China Architecture & Building Press, Beijing, 2003. (in Chinese).
[42] Powers, T. C. A working hypothesis for further studies of frost resistance of concrete. *Journal Proceedings*, Vol. 41, No. 1, 1945, pp. 245–272.
[43] Powers, T. C., and R. A. Helmuth. Theory of volume changes in hardened Portland-cement paste during freezing. *Highway Research Board Proceedings*, Vol. 36, 1953.
[44] Su, T., T. Wang, Z. Zhang, X. Sun, S. Gong, X. Mei, et al. Mechanical properties and frost resistance of recycled brick aggregate concrete modified by nano-SiO_2. *Nanotechnology Reviews*, Vol. 12, No. 1, 2023, id. 20230576.
[45] Wu, S. Y. *Effect of PVA modified recycled aggregate on properties of recycled concrete*. Anhui University of Science and Technology, Huainan, 2019. (in Chinese).

[46] Liu, L. J. *Effect of broken brick and polypropylene fiber on mechanics impermeability and frost resistance of concrete*. North China University of Water Resources and Electric Power, Zhengzhou, 2019. (in Chinese).
[47] Huo, J., C. Wang, Y. Hou, J. Wei, and P. P. Jiang. Frost resistance and pore structure of recycled fiber concrete. *Bulletin of the Chinese Ceramic Society*, Vol. 37, No. 7, 2018, pp. 2141–2145. (in Chinese).
[48] Xue, Z. and L. Li. Influence of polypropylene fiber on strength and shrinkage behaviors of concrete for pavement. *Journal of Building Materials*, Vol. 14, No. 1, 2011, pp. 132–135. (in Chinese).
[49] Li, H., H. Guo, and Y. Zhang. Deterioration of concrete under the coupling action of freeze–thaw cycles and salt solution erosion. *Reviews on Advanced Materials Science*, Vol. 61, No. 1, 2022, pp. 322–333.